# Autosomal recessive Andersen-Tawil syndrome with a novel mutation L94P in Kir2.1

Ikuko Takeda,* Tetsuya Takahashi,* Hiroki Ueno,* Hiroyuki Morino,† Kazuhide Ochi,* Takeshi Nakamura,* Naohisa Hosomi,* Hideshi Kawakami, † Kouichi Hashimoto‡ and Masayasu Matsumoto*

*Department of Clinical Neuroscience and Therapeutics, †Department of Epidemiology, Research Institute for Radiation Biology and Medicine, ‡Department of Neurophysiology, Hiroshima University, Graduate School of Biomedical and Health Sciences, Hiroshima, Japan

**Correspondence**

Tetsuya Takahashi, Department of Clinical Neuroscience and Therapeutics, Hiroshima University, Graduate School of Biomedical and Health Sciences, 1-2-3 Kasumi, Minami-ku, Hiroshima 734-8551, Japan. E-mail: tetakaha@mac.com

Tel: +81 82 257 5201; Fax: +81 82 505 0490

Running title: Autosomal recessive ATS

**Abstract**

**Aim:** Dominant negative mutations of the inwardly rectifying $K^+$ channel Kir2.1 cause Andersen-Tawil syndrome, an autosomal dominant disorder. Here, we identified a novel Kir2.1 mutation causing autosomal recessive ATS, and explored the underlying mechanism.

**Methods:** We sequenced the coding region of *KCJN2*. We assessed protein subcellular localization by transfecting cells with Kir2.1-enhanced green fluorescent protein fusions and observing them by confocal microscopy. We measured $K^+$ currents using patch clamping.

**Results:** We identified the novel Kir2.1 missense mutation L94P. L94P-EGFP was barely detected at the plasma membrane, in contrast to WT-EGFP and L94PEGFP+WT. The excitability of L94P-expressing cells was decreased compared with that of WT-expressing cells and L94P+WT-expressing cells ($p < 0.001$).

**Conclusions:** Most L94P mutant Kir2.1 fails to reach the plasma membrane, but heterotetrameric channels comprising L94P+WT can traffic normally to the plasma membrane and generate currents. The L94P mutation is transmitted as an autosomal recessive trait.

**Key Words**

Andersen-Tawil syndrome, *KCNJ2*, Kir2.1, autosomal recessive, patch clamp

## Introduction

Andersen-Tawil syndrome (ATS; OMIM# 170390) is a rare autosomal dominant disorder characterized by ventricular arrhythmias, periodic paralysis, and dysmorphic features (hypertelorism, small mandible, low-set ears, and high arched or cleft palate).

*KCNJ2*, encoding the inwardly rectifying $K^+$ channel Kir2.1 and located on chromosome 17q, is reported to be the causative gene for ATS.[1] Kir2.1 plays a critical role in stabilization of the resting membrane potential of excitable cells and the late

repolarization phase of the cardiac action potential.[2, 3] Many point mutations and two internal deletions in *KCNJ2* have been found in patients with ATS.[1, 4] The patients exhibit variable phenotypes, and some mutation carriers present little or no phenotype.[5, 6]

Some ATS mutations are attributable to defective trafficking of channel proteins to the plasma membrane,[2, 3, 7] while others reflect decreased affinity for phosphatidylinositol 4,5-bisphosphate ($PIP_2$),[4, 5]; the opening of Kir channels requires $PIP_2$ binding to their cytoplasmic domains.[8, 9] The data indicate that some mutations in *KCNJ2* cause a dominant negative effect *in vitro*. Here, we identified a novel *KCNJ2* mutation in an ATS family, which transmitted in an autosomal recessive manner. We investigated the mechanism of this mode of inheritance.

## Materials and Methods

### Clinical findings

A 62-year-old man presented initially with periodic paralysis since the age of 6. The paralysis occurred spontaneously and showed proximal weakness without myotonia. The duration of the attacks was several days to a month. Serum potassium concentration during the episodes of weakness was normal. Routine nerve conduction electrophysiology was normal but a prolonged exercise test[10] demonstrated the compound muscle action potential amplitude decrements of more than 50% that are typical of ATS. Dysmorphological features comprised short stature, low-set ears, hypertelorism, small mandible, high arched palate, dental anomalies, broad nasal root, and fifth-digit clinodactyly. Electrocardiogram showed enlarged U-waves, a wide T–U

junction, and a prolonged QUc interval (0.693 s) without a prolonged QTc interval. Holter monitoring for 24 h detected neither ventricular tachycardia nor ventricular ectopy. Flow-mediated vasodilation measured on the brachial artery as previously reported[11] was 2.0% and nitroglycerine-induced vasodilation was 19.9%. Brain MRI and magnetic resonance angiography revealed periventricular white matter lesions and right carotid artery dissection (Fig. 1A).

The proband's mother (I-2) and brother (II-1) (Fig.1B) showed no symptoms and no electrocardiogram changes typically seen in ATS. The proband's father (I-1) also did not complain of no typical symptom of ATS before he had died of cerebral infarction in his fifth decade. The parental consanguinity was not confirmed by medical interview.

**Genetic analysis of *KCNJ2***

All participants gave written consent for genetic analysis. The analysis were approved by and performed under the guidelines of the ethics committee of Hiroshima University. All the data were analyzed anonymously.

DNA was isolated from leukocyte nuclei using a QIAamp DNA Blood Maxi kit (Qiagen, Hilden, Germany). Exon 2 of *KCNJ2* (GenBank AF153820.1) was amplified with four sets of primers as follows: primer1-forward (5′-CCCCAGCAGAAGCGATGGG-3′) and reverse (5′-AACCAGCATCCACCGCCAGC-3′); primer2-forward (5′-GCTGGCGGTGGATGCTGGT-3′) and reverse (5′-GCTCATAGCGGTGGCCCCAC-3′); primer3-forward (5′-GTGGGGCCACCGCTATGAG-3′) and reverse (5′-GTCCCTTGTGGCCGCTTGCT-

3′); and primer4-forward (5′-ACGGACACGCCCCCTGACAT-3′) and reverse (5′AGTCCCTTGTGGCCGCTTGC-3′). PCR was performed with LA *Taq* DNA polymerase (TAKARA, Shiga, Japan) on a thermal cycler (ASTEC, Fukuoka, Japan). The PCR products were purified using a PCR Product Purification kit (Medical & Biological Laboratories Co., Aichi, Japan). The products were sequenced in both directions and resolved using an ABI PRISM 310 Genetic Analyzer (Applied Biosystems, Foster City, CA). CytoScan HD Solution (Affymetrix, Snta Clara, CA) was used for DNA copy number and areas of loss of heterozygosity. The results was analysis by the Affymetrix Chromosome Analysis Suite (ChAS) software. Percentage of homozygosity was calculated by summing ROH > 5 Mb across the covered autosome ( 2,578,427,245 bps for CytoScan) as previously described.[12] The mutation has been submitted to a database based on the Leiden Open Variation Database and accessible at www.lovd.nl/kcnj2. Lipophilicity of the transmembrane region was calculated using the empirical scoring function LIPS (LIPid-facing Surface) (http://tanto.bioengr.uic.edu/lips/).[13]

**Expression of *KCNJ2***

PCR was performed with Pfu Ultra High Fidelity DNA polymerase (Agilent Technologies, Santa Clara, CA). Wild-type (WT) and mutant (L94P) PCR products were digested with EcoR I and Sal I and were subcloned into pEGFP-N3 (Clontech, Mountain View, CA) or digested with BamH I and Xho I and subcloned into pcDNA3 (Life Technologies, Carlsbad, CA). The complete *KCNJ2* coding region was sequenced in all constructs for verification.

**Cell culture and transfection**

CHO-K1 cells (Health Science Research Resources Bank, Osaka, Japan) were used for whole cell recordings because of their low level of endogenous $K^+$ currents, and human embryonic kidney 293 (HEK293) cells (Health Science Research Resources Bank) were used for immunostaining and the plasma membrane sheet assay. CHO-K1 cells were cultured in Ham medium (Wako Pure Chemical Indusries, Osaka, Japan) with 10% fetal bovine serum. HEK293 cells were cultured in Dulbecco's modified Eagle's medium (Life Technologies) with 10% fetal bovine serum. For expression of WT and mutant Kir2.1, CHO-K1 and HEK293 cells were transfected with 2 μg of WT- or L94Penhanced green fluorescent protein (EGFP) fusion protein using X-tremeGENE 9 transfection reagent (Roche, Indianapolis, IN). For co-expression of WT and mutant protein, cells were transfected with 1 μg L94P-EGFP and 1 μg WT (WT-EGFP or pcDNA3-WT).

**Immunostaining and microscopy**

Immunocytochemistry for membrane inositol lipids was performed as previously described.[14] Twenty-four hours after transfection, the cells were chilled for 2 minutes then fixed with 4% paraformaldehyde and 0.2% glutaraldehyde for 15 minutes. The cells were blocked and permeabilized with 10% goat serum and 0.5% saponin for 45 minutes on ice. Then, the cells were incubated with mouse anti-$PIP_2$ antibody (2C11, 1:50; Santa Cruz Biotechnology, Santa Cruz, CA). The cells were then washed and incubated with anti-mouse antibody conjugated to Alexa Fluor 568 (1:200; Life

Technologies). To minimize the cell surface, CHO-K1 cells transfected with Kir2.1EGFP were observed on coverslips after being stripped from the dishes by treatment with 0.25% trypsin for 30 s and resuspended in phosphate-buffered saline (PBS).[15] The cells were examined by confocal laser scanning microscopy (Olympus, Tokyo, Japan) with a 60× oil immersion objective lens.

**Plasma membrane sheet assay**

The plasma membrane sheet assay was used to obtain plasma membrane lawns.[16] HEK293 cells were washed in PBS, followed by a 20–30-s treatment with 0.5 mg/ml poly L-lysine in PBS. The cells were washed three times in 1/3× KHMgE (30 mM HEPES, 70 mM KCl, 5 mM $MgCl_2$, 3 mM EGTA, pH7.4). The cells were then sonicated in Buzz solution (1× KHMgE, 1 mM dithiothreitol, 1 mM phenylmethylsulfonyl fluoride) and washed three times in Buzz solution. Following the isolation of plasma membrane sheets, the membranes were scraped into sample buffer. Primary antibodies–rabbit anti-GFP (1:2000; Life Technologies) and rabbit anti-caveolin 1 (1:1000; Cell Signaling, Danvers, MA)–were added to the solution. Subsequently, immunocomplexes were visualized using a secondary antibody–goat antirabbit, HRP conjugated (1:5000; Santa Cruz Biotechnology) and chemiluminescent detection.

**Electrophysiology**

Whole-cell recordings were made from GFP-expressing CHO-K1 cells using an upright microscope (BX51WI; Olympus) at room temperature. Co-transfection was performed with L94P-EGFP + pcDNA3-WT. Untransfected CHO-K1 cells in each dish

were used as controls. Ionic currents were recorded with an EPC-10 patch clamp amplifier (HEKA Elektronik, Lambrecht/Pfalz, Germany). The resistances of the patch pipettes were 2–3 M when filled with an intracellular solution composed of: 130 mM D-glutamate, 15 mM KCl, 5 mM NaCl, 10 mM HEPES, 0.5 mM EGTA, and 4 mM MgATP (pH 7.3, adjusted with KOH). The composition of the standard bathing solution was: 125 mM NaCl, 2.5 mM KCl, 2 mM $CaCl_2$, 1 mM $MgSO_4$, 1.25 mM $NaH_2PO_4$, 26 mM $NaHCO_3$ and 20 mM glucose, bubbled with 95% $O_2$ and 5% $CO_2$ (pH 7.4). The holding potential was not corrected for the liquid–junction potential. The signals were filtered at 2 kHz and digitized at 20 kHz. The currents were recorded during voltage ramp (holding potential (hp) of +60 to –150 mV, 2 s). Online data acquisition and offline data analysis were performed using PatchMaster software (HEKA Electronik).

**Statistical analysis**

Comparisons were made using analysis of variance and Dunnett's test. Values of $p < 0.05$ were considered significant. All values are reported as mean ± standard error.

**Results**

**Identification of *KCNJ2* mutation in a family**

A novel mutation c.281T>C was identified in the proband (II-3) and the proband's mother (I-2) (Fig. 1B and C). The mutation, which would substitute leucine for proline (p.Leu94Pro), was located in an -helix that forms the outer transmembrane region M1 (Fig. 1D). Leucine at residue 94 is highly conserved across species (Fig. 1E)

and is one of the nine lipid-facing residues located in helix M1.[17] Leucine is a hydrophobic amino acid that is important for protein–bilayer interactions and membrane protein folding. The average helical-face lipophilicity score for WT M1 was 3.182, whereas that for L94P was 2.989, which is smaller than that for another helical-face residue in M1 (3.113). The mutation was present in a homozygous state in the proband (II-3). The proband's asymptomatic mother (I-2) had the same mutation in a heterozygous state. Direct sequencing of *KCNJ2* from the proband and his family revealed no other mutations. CytoScan identified 11.4 Mb (region from 66813807 to78212206) of the region of homozygosity on chromosome 17 containing *KCNJ2* (Fig. 2). The regions of homozygosity > 5 Mb covered 3.4% of the autosome. CytoScan revealed large regions of homozygosity that suggest identity by descent.[12] The L94P substitution was not observed in 146 unaffected Japanese and not registraedin dbSNP 137 (Jun 26, 2012).

**Subcellular distribution**

Confocal microscopy imaging was performed to investigate the channel distribution in HEK293 cells. We examined the localization of Kir2.1 in relation to that of $PIP_2$ that interacts with Kir2.1 at plasma membranes. WT-EGFP was expressed at the plasma membrane and colocalized with $PIP_2$ (Fig. 3A). In contrast, L94P-EGFP was only faintly expressed at the plasma membrane, and was mainly localized in the cytoplasm (Fig. 3A). The cell surface expression of L94P-EGFP channel proteins was

increased by co-expression with WT (Fig. 3A). To clarify the subcellular transport of Kir2.1, we examined the localization of EGFP in HEK293 cells that had been stripped from the dishes (Fig. 3B). The line intensity histograms showed that WT-EGFP and L94P-EGFP co-transfected with pcDNA3-WT gave strong signals at the plasma membrane. However, L94P-EGFP signals alone were weak at the plasma membrane. We then used a plasma membrane sheet assay to evaluate the expression levels of the Kir channel at the plasma membrane. Proteins extracted from HEK293 cells transfected with WT-EGFP, L94P-EGFP, or L94P-EGFP+WT-EGFP were analyzed using an antiGFP antibody. The assay detected less L94P-EGFP protein than WT-EGFP or L94PEGFP+WT-EGFP proteins at the plasma membrane (Fig. 3C). These results suggest that WT subunits can form heterotetramers with L94P subunits and be recruited to the plasma membrane.

**Electrophysiological analysis**

Finally, we investigated the effects of the L94P mutation on the properties of the Kir2.1 channel. CHO-K1 cells were transfected with WT-EGFP (2 μg), L94P-EGFP (2 μg), or L94P-EGFP (1 μg) +pcDNA3-WT (1 μg). Inwardly rectifying currents that reversed around the equilibrium potential of $K^+$ could be recorded from cells expressing WT-EGFP (Fig. 4A), as reported previously.[18] In contrast, the currents were significantly weaker in the cells expressing L94P-EGFP (–332.9 ± 47.9 pA) than in those expressing WT-EGFP (–2217.4 ± 337.4 pA at hp = –150 mV; $p < 0.001$) (Fig. 4A, B). This result may be consistent with our evidence indicating reduced translocation of mutant Kir2.1 to the plasma membrane (Fig. 3A). Inwardly-rectifying currents were observed in cells co-

expressing both L94P-EGFP and WT. The current amplitude in these cells (–1482.6 ± 304.1 pA at hp = –150 mV) was about 67% of that in cells expressing WT-EGFP (Fig. 4A), but the difference was not significant ($p = 0.099$) (Fig. 4B). These results suggest that the L94P mutation does not have a severe dominant negative effect on the WT protein.

**Discussion**

We identified a novel Kir2.1 L94P mutation in a patient with ATS that reduced protein trafficking to the plasma membrane. The large regions of homozygosity on the autosome suggest parental consanguinity and autosomal recessive inheritance. Kir2.1 channel has outer and inner transmembrane helix domains called M1 and M2, respectively, and the N-terminus and C-terminus form the cytoplasmic domains. The $PIP_2$-binding residues of Kir2.1 located in the cytoplasmic domain are the most common targets for mutation.[5] $PIP_2$ binding with the cytoplasmic domain induces a conformational change that induces channel opening.[19] The L94 residue in the M1 segment faces the lipid bilayer[17] and does not communicate with $PIP_2$. Increasing lines of evidence indicate that trafficking-defective mutant proteins (Δ95–98, C101R, Δ314–315, and S369X) are incapable of reaching the plasma membrane by themselves.[2, 3, 7] Because the C-terminus of Kir2.1 is necessary to promote the export from the ER[20] and/or the Golgi apparatus,[21, 22] lack of export motifs in C-terminus induced by Δ314–315 and S369X causes trafficking defect. Δ95–98 and C101R are located in M1, like L94P. The Δ95–98 protein is trapped in the cytoplasm even when it is co-transfected with WT protein. C101R is also indicated to be a trafficking-defective mutation.[3] While

Δ95–98 causes misfolding of the protein and retention in the ER or degradation, L94P may have the ability to co-localize with the WT protein in the plasma membrane. S369X mutant protein co-transfected with WT could be transported to the membrane and form functional channels.[7] L94P is similar to S369X in that these mutants do not exhibit dominant negative effects on the WT protein.

The L94 residue faces the lipid bilayer.[17] The Kir channel transmembrane helix structures are based on the prokaryotic homologs of Kir channels KirBac structure, because they all have two transmembrane helix domains. The mutation of G77 in Kir4.1 (G77R) that corresponds to L94 in Kir2.1[17] shows a reduction of surface expression in vitro and an autosomal recessive pattern in inheritance[23] as does L94P. The authors suggested that the replacement of glycine with arginine in this mutation would be unfavorable in the lipid bilayer. Leucine has a large side chain and is strongly hydrophobic; conversely, proline has a small non-polar side chain and is weakly hydrophobic. High lipophilicity of the lipid-facing region in a transmembrane helix is required to retain it in the lipid bilayer.[24] Replacement of a leucine with a proline is predicted to change the lipophilicity and may disrupt protein stability in the plasma membrane. Upon delivery to the plasma membrane, the L94P/WT heterotetramer could elicit an inward current. These characteristics might be associated with autosomal recessive inheritance.

Hereditary variation in channelopathies is also reported for the voltage-gated chloride channel. Myotonia congenita, caused by chloride channel gene mutations, expresses as autosomal dominant myotonia congenita (Thomsen's disease) or autosomal

recessive myotonia congenita (Becker's disease). In dominant myotonia congenita, one well-accepted mechanism is that mutations located at or near the heterodimer interface of the chloride channel cause a dominant negative effect on the function of the gate.[25, 26] Conversely, the recessive form of myotonia congenita is diverse in its mechanisms. Among these, a recent report demonstrated two mutations related to trafficking defects.[27] Both mutations were situated in a membrane-spanning segment of the transmembrane region. One of the mutant channels was functional when delivered to the plasma membrane.

Kir2.1 is expressed not only in excitable cells such as neurons, skeletal muscle, and cardiac muscle but also in endothelial cells. In endothelial cells, Kir2.1 is required for the response to shear stress.[28] In our proband, flow-mediated vasodilation was reduced but nitroglycerine-mediated vasodilation was preserved, indicative of an impairment of endothelial-dependent vasodilatation probably caused by poor sensitivity to shear stress, at least in part. In addition, a recent study has suggested that a mutation in the *Drosophila* homolog of Kir2.1 disrupts the function of bone morphogenetic protein (BMP), part of the transforming growth factor β (TGFβ)/BMP signaling pathway, and causes morphological abnormalities similar to ATS.[29] Because TGFβ/BMP signaling also controls vascular morphogenesis and extracellular matrix synthesis,[30] patients with Loeys-Dietz syndrome, caused by impairment of TGFβ/BMP signaling, have a risk of aortic dissection. The L94P mutation in Kir2.1 might be a cause of the asymptomatic carotid artery dissection in this proband via disruption of TGFβ/BMP signaling.

In summary, the Kir2.1 mutation L94P shows a reduction of surface expression in vitro and an autosomal recessive pattern in inheritance. These findings provide insight into the molecular mechanisms underlying different modes of inheritance of a human clinical condition of the nervous system. Moreover, our methods and hypotheses may be applicable to the study of other channelopathies.

**Acknowledgements**

We thank the patients for their kind participation. We are grateful to Mr. Y. Nagano, Ms. Y. Furuno and Mr. K. Shimamoto for their technical assistance, and Ms. N. Morihara for her help in Affymetrix chromosome analysis. This work was carried out at the Analysis Center of Life Science, Natural Science Center for Basic Research and Development, Hiroshima University. This work was supported by a grant from the Japanese Ministry of Education, Culture, Sports, Science, and Technology to Ueno and a grant from the Smoking Research Foundation, Tokyo, Japan.

**References**


1. Plaster NM, Tawil R, Tristani-Firouzi M*, et al.* Mutations in Kir2.1 cause the developmental and episodic electrical phenotypes of Andersen's syndrome. *Cell* 2001; **105**: 511-9.
2. Bendahhou S, Donaldson MR, Plaster NM, Tristani-Firouzi M, Fu YH, Ptacek LJ. Defective potassium channel Kir2.1 trafficking underlies Andersen-Tawil syndrome. *J Biol Chem* 2003; **278**: 51779-85.
3. Ballester LY, Benson DW, Wong B*, et al.* Trafficking-competent and traffickingdefective KCNJ2 mutations in Andersen syndrome. *Hum Mutat* 2006; **27**: 388.
4. Lopes CM, Zhang H, Rohacs T, Jin T, Yang J, Logothetis DE. Alterations in conserved Kir channel-PIP2 interactions underlie channelopathies. *Neuron* 2002; **34**: 933-44.
5. Donaldson MR, Jensen JL, Tristani-Firouzi M*, et al.* PIP2 binding residues of Kir2.1 are common targets of mutations causing Andersen syndrome. *Neurology* 2003; **60**: 1811-6.
6. Tristani-Firouzi M. Andersen-Tawil syndrome: an ever-expanding phenotype? *Heart Rhythm* 2006; **3**: 1351-2.
7. Doi T, Makiyama T, Morimoto T*, et al.* A novel KCNJ2 nonsense mutation, S369X, impedes trafficking and causes a limited form of Andersen-Tawil syndrome. *Circ Cardiovasc Genet* 2011; **4**: 253-60.

8. D'Avanzo N, Cheng WW, Doyle DA, Nichols CG. Direct and specific activation of human inward rectifier K+ channels by membrane phosphatidylinositol 4,5bisphosphate. *J Biol Chem* 2010; **285**: 37129-32.

9. Xie LH, John SA, Ribalet B, Weiss JN. Activation of inwardly rectifying potassium (Kir) channels by phosphatidylinosital-4,5-bisphosphate (PIP2): interaction with other regulatory ligands. *Prog Biophys Mol Biol* 2007; **94**: 320-35.

10. Katz JS, Wolfe GI, Iannaccone S, Bryan WW, Barohn RJ. The exercise test in Andersen syndrome. *Arch Neurol* 1999; **56**: 352-6.

11. Fujii Y, Teragawa H, Soga J*, et al.* Flow-Mediated Vasodilation and Anatomical Variation of the Brachial Artery (Double Brachial Artery) in Healthy Subjects and Patients With Cardiovascular Disease. *Circulation Journal* 2012.

12. Sund KL, Zimmerman SL, Thomas C*, et al.* Regions of homozygosity identified by SNP microarray analysis aid in the diagnosis of autosomal recessive disease and incidentally detect parental blood relationships. *Genetics in Medicine* 2012; **15**: 70-8.

13. Adamian L, Liang J. Prediction of transmembrane helix orientation in polytopic membrane proteins. *BMC Struct Biol* 2006; **6**: 13.

14. Hammond GR, Schiavo G, Irvine RF. Immunocytochemical techniques reveal multiple, distinct cellular pools of PtdIns4P and PtdIns(4,5)P(2). *Biochem J* 2009; **422**: 23-35.

15. Makhina EN, Nichols CG. Independent trafficking of KATP channel subunits to the plasma membrane. *J Biol Chem* 1998; **273**: 3369-74.

16. Robinson LJ, James DE. Insulin-regulated sorting of glucose transporters in 3T3-L1 adipocytes. *Am J Physiol* 1992; **263**: E383-93.

17. Bichet D, Haass FA, Jan LY. Merging functional studies with structures of inwardrectifier K(+) channels. *Nat Rev Neurosci* 2003; **4**: 957-67.

18. He Y, Xiao J, Yang Y*, et al.* Stretch-induced alterations of human Kir2.1 channel currents. *Biochem Biophys Res Commun* 2006; **351**: 462-7.

19. Rapedius M, Fowler PW, Shang L, Sansom MS, Tucker SJ, Baukrowitz T. H bonding at the helix-bundle crossing controls gating in Kir potassium channels. *Neuron* 2007; **55**: 602-14.

20. Ma D, Zerangue N, Lin YF*, et al.* Role of ER export signals in controlling surface potassium channel numbers. *Science* 2001; **291**: 316-9.

21. Hofherr A, Fakler B, Klocker N. Selective Golgi export of Kir2.1 controls the stoichiometry of functional Kir2.x channel heteromers. *J Cell Sci* 2005; **118**: 1935-43.

22. Ma D, Taneja TK, Hagen BM*, et al.* Golgi export of the Kir2.1 channel is driven by a trafficking signal located within its tertiary structure. *Cell* 2011; **145**: 1102-15.

23. Williams DM, Lopes CM, Rosenhouse-Dantsker A*, et al.* Molecular basis of decreased Kir4.1 function in SeSAME/EAST syndrome. *J Am Soc Nephrol* 2010; **21**: 2117-29.

24. Rees DC, DeAntonio L, Eisenberg D. Hydrophobic organization of membrane proteins. *Science* 1989; **245**: 510-3.

25. Duffield M. Involvement of Helices at the Dimer Interface in ClC-1 Common

Gating. *The Journal of General Physiology* 2003; **121**: 149-61.

26. Pusch M. Myotonia caused by mutations in the muscle chloride channel gene CLCN1. *Hum Mutat* 2002; **19**: 423-34.
27. Papponen H, Nissinen M, Kaisto T, Myllyla VV, Myllyla R, Metsikko K. F413C and A531V but not R894X myotonia congenita mutations cause defective endoplasmic reticulum export of the muscle-specific chloride channel CLC-1. *Muscle Nerve* 2008; **37**: 317-25.
28. Hoger JH, Ilyin VI, Forsyth S, Hoger A. Shear stress regulates the endothelial Kir2.1 ion channel. *Proc Natl Acad Sci U S A* 2002; **99**: 7780-5.
29. Dahal GR, Rawson J, Gassaway B*, et al.* An inwardly rectifying K+ channel is required for patterning. *Development* 2012; **139**: 3653-64.
30. Jaffe M, Sesti C, Washington IM*, et al.* Transforming growth factor-beta signaling in myogenic cells regulates vascular morphogenesis, differentiation, and matrix synthesis. *Arterioscler Thromb Vasc Biol* 2012; **32**: e1-11.

**Figure Legends**

**Fig. 1 Clinical findings and ATS mutations**

A: Magnetic resonance angiography showed right carotid artery dissection in the proband (arrowhead).

B: Pedigree of the ATS family. The proband is indicated by P. Genotype is indicated by "+", mutated allele and "-", wild-type allele.

C: Sequence chromatogram of part of the *KCNJ2* gene. The arrows show the position c.281, of the mutation that would alter the coding sequence from leucine to proline (L94P mutation).

D: Structure of Kir2.1. The locations of known mutations in Kir2.1 are represented on the structure (previous reports, black; this report, red). M1 and M2 indicate transmembrane regions.

E: Alignment of the amino acid sequence of Kir2.1 flanking L94P in *Homo sapiens* (NP_000882.1), *Oryctolagus cuniculus* (NP_001075667.1), *Rattus norvegicus* (NP_058992.1), *Mus musculus* (NP_032451.1), *Gallus* (NP_990701.1), *Drosophila melanogaster* (NP_732871.1), and *Caenorhabditis elegans* (NP_509138.2). Dots represent an identical amino acid to that at the same position in *Homo sapiens*.

**Fig. 2. The region of homozygosity on chromosome 17**

The blue line represents copy number. There was no copy number variations on chromosome 17. The blue bar indicates the region of homozygosity. The allele difference graph represents the genotypes for each individual alleles. Each blue dot with a value of 1 represent alleles with an "AA"genotype, while those with a value of -1

represent alleles with a “BB” genotype. Blue dots at 0 represent heterozygous alleles (“AB”). Dot line (black arrow) indicates the region of *KCNJ2*.

**Fig. 3. Distribution of Kir2.1-EGFP in HEK293 cells**

(A, B) Confocal microscopic images of HEK293 cells transfected with WT-EGFP (a), L94P-EGFP (b), or L94P-EGFP+pcDNA3-WT (c).

A. Plasma membranes were stained with anti-$PIP_2$ antibody. Scale bars = 10 μm.

B. The cells were treated with trypsin. The lower panels show the corresponding GFP intensity profiles, detected along the red lines. Scale bars = 5 μm.

C. Proteins from the plasma membranes of HEK293 cells transfected with WT-EGFP, L94P-EGFP, or L94P-EGFP+WT-EGFP were analyzed by western blotting using an anti-GFP antibody. Caveolin 1 was used as a marker of the plasma membrane.

**Fig. 4. Electrophysiological analysis**

A: I–V relationships of averaged currents recorded during a voltage ramp from CHO-K1 cells transfected with WT-EGFP ($n$ = 16), L94P-EGFP ($n$ = 16), or L94PEGFP+pcDNA3-WT ($n$ = 16). Currents were measured during voltage ramp from +60 mV to –150 mV (duration, 2 s). Averaged currents from untransfected CHO-K1 cells in each dish were recorded as controls (untransfected-WT: $n$ = 17, untransfected-L94P: $n$ = 16, untransfected-L94P+WT: $n$ =17). Error bars represent the standard error at (from left to right) –137.5, –125, –112.5, –100, –87.5, –75, –67.5, –50, –37.5, –25, –12.5, 0,

12.5, 25, and 37.5 mV.

B: Histogram of averaged currents measured at –150 mV in CHO-K1 cells. Bars indicate the mean ± standard error of the current amplitudes. The three groups were significantly different ($p < 0.001$) by analysis of variance. *$p < 0.001$ by Dunnett's test.

**Fig. 1.**

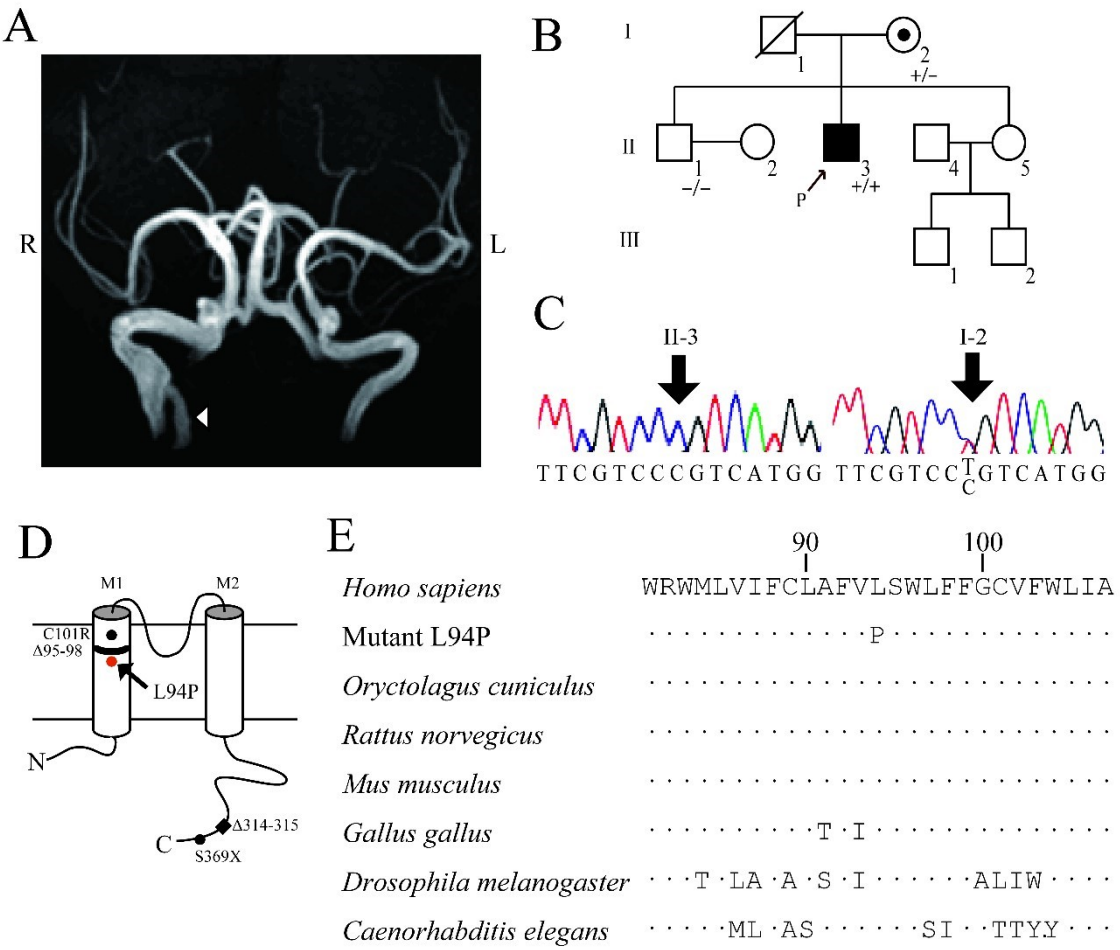


**Fig. 2.**

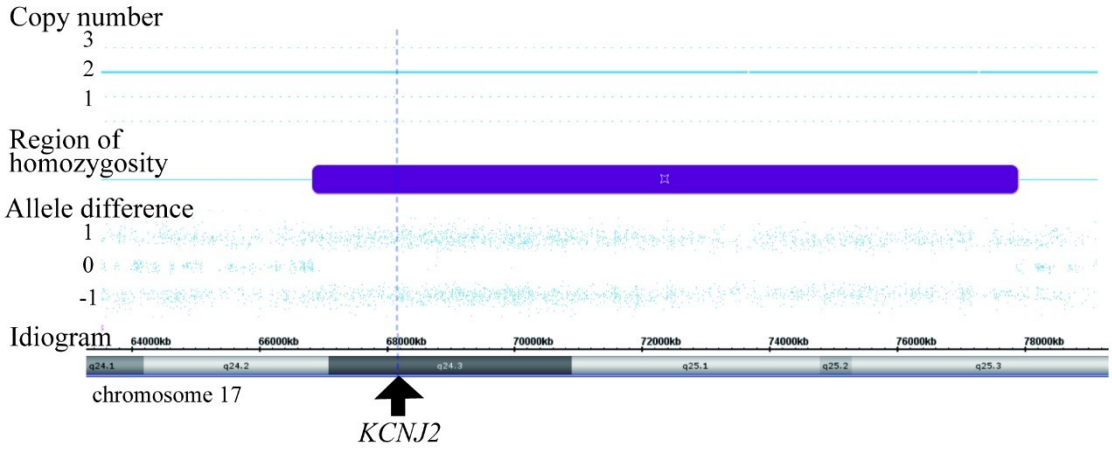
Copy number
3
2
1
Region of homozygosity
Allele difference
1
0
-1
Idiogram
64000kb
66000kb
68000kb
70000kb
72000kb
74000kb
76000kb
78000kb
q24.1
q24.2
q24.3
q25.1
q25.2
q25.3
chromosome 17
KCNJ2

**Fig. 3.**

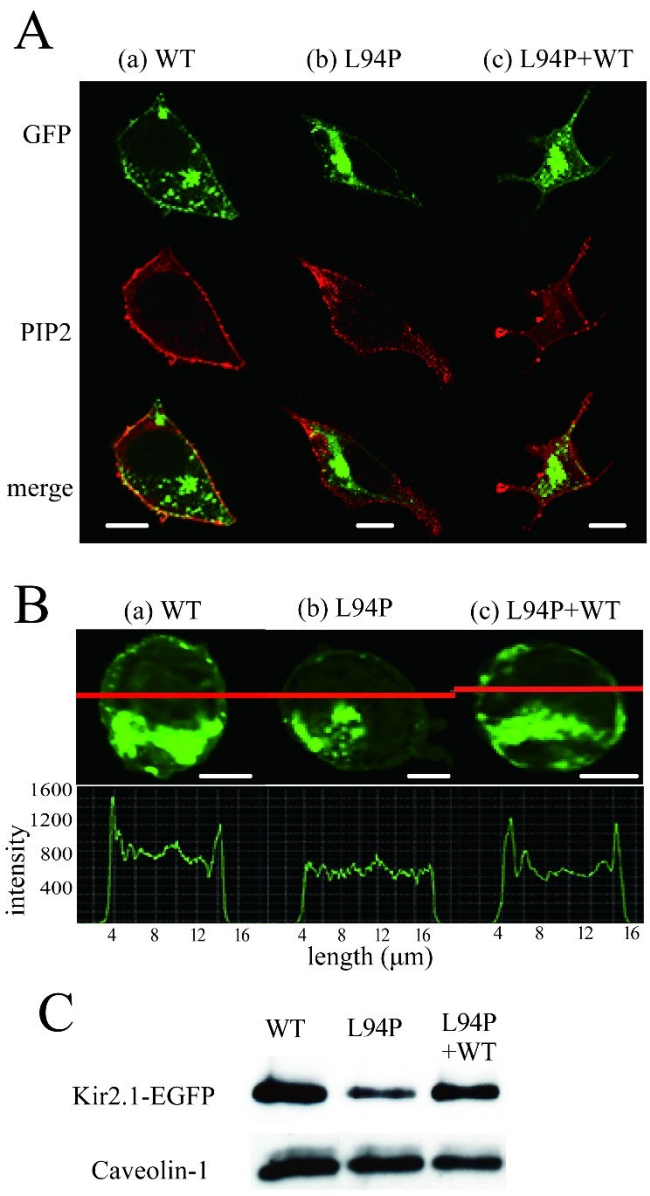
A
(a) WT
(b) L94P
(c) L94P+WT
GFP
PIP2
merge
B
(a) WT
(b) L94P
(c) L94P+WT
1600
1200
800
400
intensity
4 8 12 16 4 8 12 16 4 8 12 16
length (μm)
C
WT
L94P
L94P
+WT
Kir2.1-EGFP
Caveolin-1

**Fig. 4.**

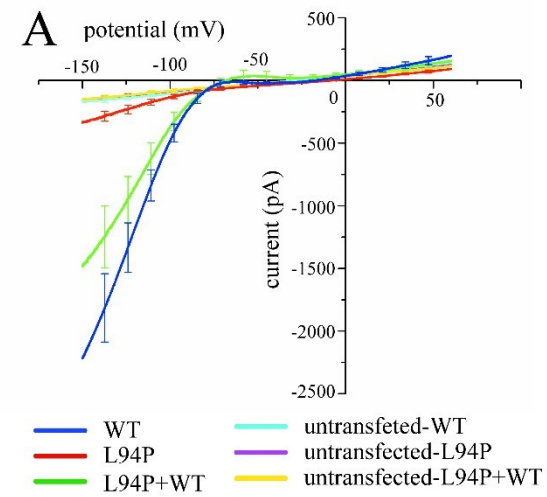
A
potential (mV)
-150
-100
-50
0
50
500
-500
-1000
-1500
-2000
-2500
current (pA)
WT
L94P
L94P+WT
untransfeted-WT
untransfected-L94P
untransfected-L94P+WT

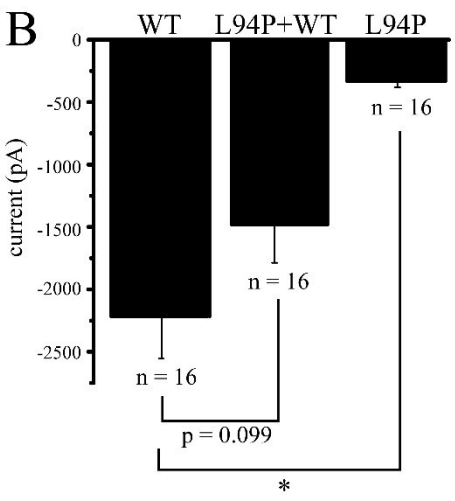
B
WT
L94P+WT
L94P
0
-500
-1000
-1500
-2000
-2500
current (pA)
n = 16
n = 16
n = 16
p = 0.099
*

This is the pre-peer-reviewed version of the following article: Ikuko Takeda, Tetsuya Takahashi, Hiroki Ueno, Hiroyuki Morino, Kazuhide Ochi, Takeshi Nakamura, Naohisa Hosomi, Hideshi Kawakami, Kouichi Hashimoto and Masayasu Matsumoto. Autosomal recessive Andersen-Tawil syndrome with a novel mutation L94P in Kir2.1. *Neurology and Clinical Neuroscience* 2013; **1**: 131-137, which has been published in final form at http://onlinelibrary.wiley.com/doi/10.1111/ncn3.38/abstract.